A Self-Powered Early Warning Glove with Integrated Elastic-Arched Triboelectric Nanogenerator and Flexible Printed Circuit for Real-Time Safety Protection

Lulu Zu, Di Liu, Jiajia Shao, Yuan Liu, Sheng Shu, Chengyu Li, Xue Shi, Baodong Chen,* and Zhong Lin Wang*

A matched and self-powered supply for a variety of wearable electronics remains a critical challenge. Here, a fully self-powered early warning glove (SEWG) is developed via unique elastic-arched triboelectric nanogenerator (EA-TENG) and flexible printed circuit technology. The EA-TENG generates electricity from a continuous touch lightly by hand or body, as a sustainable self-powered source that can be utilized to complete one charging process by simply five times slapping. The SEWG has the advantage that can really deliver real-time no-contact electrostatic monitoring when no external power is supplied, and can effectively avoid the electric shock accident in 220/380 V electric maintenance work. Quantitative analysis of the mechanical and electronic characteristics of the SEWG demonstrated its advantages in terms of stability and reliability, with consistently well performance over more than 80,000 working cycles. It is anticipated that the special design of integrated self-powered system could produce more implications in the field of wearable/flexible electronics and human-machine interaction.

1. Introduction

Wearable electronics deal with anything products that can be worn on the body which implement electronic and computing

L. Zu, D. Liu, J. Shao, Y. Liu, S. Shu, C. Li, X. Shi, B. Chen, Z. L. Wang
Beijing Institute of Nanoenergy and Nanosystems
Chinese Academy of Sciences
Beijing 101400, P. R. China
E-mail: chenbaodong@binn.cas.cn; zlwang@gatech.edu
L. Zu, D. Liu, J. Shao, Y. Liu, S. Shu, C. Li, X. Shi, B. Chen, Z. L. Wang
School of Nanoscience and Technology
University of Chinese Academy of Sciences
Beijing 100049, P. R. China
B. Chen
Institute of Applied Nanotechnology
Jiaxing, Zhejiang 314031, P. R. China
Z. L. Wang
CUSTech Institute
Wenzhou, Zhejiang 325024, P. R. China
Z. L. Wang
School of Materials Science and Engineering
Georgia Institute of Technology
Atlanta, GA 30332-0245, USA

devices within their everyday functionality, which is a relatively whole new field of research which has begun to strongly catch hold within the high-technology community. This is due to rapid electronic, computing, and integrated techniques advances that have been made in the last decade. In recent years, it was considered that the trend for electronic devices has been to be lighter, thinner, smaller, and softer.[1–3] Flexible electronics are regarded as the next revolutionary technology for advanced electronics because of its excellent electrical performance and flexibility.[4] Once the electronics can adapt to the deformation demands of different environments, they can be utilized in a wider range of applications such as wearable electronics,[5] human–machine interfaces,[6,7] flexible displays,[8] healthcare,[9] electronic skin,[10,11] radio frequency identification,[12] etc. Compared with traditional printed circuit board manufacturing technology, the circuit made by additive manufacturing (AM) technology has the advantages of simplicity, speed, and cost. Printed electronics (PE) is an emerging sector under AM, which uses functional inks to print circuits and sensors on various substrates.[13] Flexible electronics manufactured by PE technology are revolutionizing the field of wearable devices through fast integration and portable solutions. Meanwhile, healthy, medical rehabilitated, academic, and mainstream consumer markets are all areas currently exploring both the popularity and usefulness of wearable electronics. However, the urgent demand of the power supply has been triggered by the development of wearable electronics.[14–16] To achieve continuous and long-term power supply for wearable electronics to form a flexible self-powered system is a huge challenge to the existing power technology.[17] A matched power supply with flexible, adaptive, and sustainable functions is a key link in the realization of wearable self-powered systems.[18–20]

Since 2012, the triboelectric nanogenerator (TENG), using Maxwell's displacement current as the driving force, has been invented by Wang et al., which can effectively convert mechanical energy into electricity.[21] Compared with conventional rigid batteries, which cannot bypass the repetitive recharging and replacing processes, a TENG can harvest environmental mechanical energy from human body motion and serve as a

ADVANCED
SCIENCE NEWS
www.advancedsciencenews.com

ADVANCED
MATERIALS
TECHNOLOGIES
www.advmattechnol.de

high-efficiency energy source for flexible-wearable electronic devices.[22,23] In addition, the TENG also has the advantages of light weight, low cost, versatile material, simple production, and environmental friendliness, making it to be a powerful alternative as a reliable power supply system for wearable electronic devices.[24] With the rapid development of wearable electronic devices, TENG as one of the most promising area attracts a lot of attention, by which people intend to solve the challenges encountered in the field of flexible circuit.[25,26] Wang et al. constructed a flexible tubular TENG array, which was placed on the sole of shoes to convert the mechanical energy of human walking into electricity to power electronic devices such as LEDs and electronic watches.[27] Zou et al. reported a bionic stretchable TENG integrated into a wetsuit for underwater energy harvesting and human motion monitoring.[28] It can be seen that in this era of rapid development of the Internet of Things and various flexible-wearable electronics, the self-powered system led by TENG has tremendous potentialities.[29–32]

In this work, a fully self-powered early warning glove (SEWG) was developed, which was composed of the core component of the elastic-arched triboelectric nanogenerator (EA-TENG) based on contact-separation mode, a flexible printed circuit, and a pair of insulate gloves. The SEWG can be utilized as both a mechanical energy harvester and a soft self-powered source for the electrostatic detection and no-contact, early warning sensing system to avoid the electric shock accident. On the one hand, the EA-TENG generates electricity from a continuous touch lightly by hand or body, as a sustainable self-powered source that can be utilized to complete one charging process by simply five times slapping. Regardless of whether it is a low-voltage range of 220/380 V or a high-voltage level of more than 1 kV of human body static electricity, the SEWG will indicate an ALARM/NORMAL condition via LED to avoid the direct contact with an energized conductor, owing to the sufficient detection range. On the other hand, we have studied its performance under different structures and temperature and humidity environments, and the results are quite satisfactory. Quantitative analyses of the mechanics and electronics characteristics of the glove demonstrate advantages in stability and reliability, which there is always a well output performance when is operated more than 80 000 working cycles. Thereby indicating that the design of the SEWG is reliable for practical applications, and has benefits of simple operation, and preventing many injuries to the hand and body. So that, implies EA-TENG a breakthrough has been made for energy harvesting of human activities and self-powered sensing system, and may be of certain reference significance on the development of self-powered wearable device in near future.

2. Result and Discussion

2.1. Design and Overview of the SEWG

The overall design and typical usage scenarios of fabricated SEWG are shown in **Figure 1**a, and each component is placed in a way that optimizes signal acquisition. The flexible coil that detects signal are located above the tip of the index finger of

the glove, the LED indicator is placed at the back of hand hid in gloves' interlayer, and the EA-TENG is positioned on the wrist to the benefit of harvesting biomechanical energy from hand. The advantages of such an integrated arrangement are that not only does it not affect the flexibility of the operator when working with gloves, but it will simplify the operation of detection and play a protective role. When the finger part of the SEWG is close to the AC charged object, the electric signal will be immediately transmitted through a series of components, and released by the LED indicator to warn the user. The integrated process of flexible printed circuit is shown in Figure 1b, where circuit fabricated on polyethylene terephthalate (PET) substrate by ink-jet printing are integrated with surface mounted devices (SMD) components into a flexible sensing platform. The silver inks serve as electrical interconnects between SMD, due to their characteristics of outstanding electrical conductivity and high chemical resistance. Each SMD's pins are mounted precisely onto the rectangular electrode pads, different from PCBs which have need of welding with tin, conductive silver glue is the connector between the SMDs and the electrode printed by silver inks. Figure 1c provides an exploded view of the EA-TENG, which consists of PET substrate used to maintain with the elastic-arched structure, fluorinated ethylene propylene (FEP) dielectric material as one of the friction layer and copper foil as both of the other friction layer and electrode. The shape of the EA-TENG can be well reshaped because of the PET tape's tension, in which the device equipped with well contact and separation characters. EA-TENG acts as an energy source to power the back-end circuit without the need for other power sources, so the whole circuit can be self-powered. The flexible circuit of the SEWG incorporates two working modules: i) energy harvesting module (Figure 1d, top right), and ii) signal acquisition and alarm module (Figure 1d, bottom right). The flexible circuit provides an excellent combination of electrical conductivity and softness that can change its shape following with hand's detected motion (Figure 1e).

2.2. Working Mechanism of the EA-TENG

The working mechanism of the EA-TENG is demonstrated in **Figure 2**a. First, the FEP film and the top copper foil will contact each other when EA-TENG is transformed by being pressed. Negative triboelectric charges are gained by the FEP due to its stronger ability to trap negative charges, while copper leaves positive charges behind (state i). Then, as the force is being removed, the transformed EA-TENG will have a tendency to rebound because of elastic recovery of the substrate. The separation between the FEP film and top electrode creates an electric potential difference between the two electrodes, thereby driving free electrons to flow from the bottom electrode to the top one (state ii). The current is generated until EA-TENG returns to its original shape (state iii). When FEP film and the top electrode get close to each other again, the top electrode will be induced to produce the opposite charges to the FEP film. Therefore, free electrons flow back from the top electrode to the bottom one, creating a reverse current flow (state iv). By repeating the contact-separation movement between two triboelectric layers, the periodic
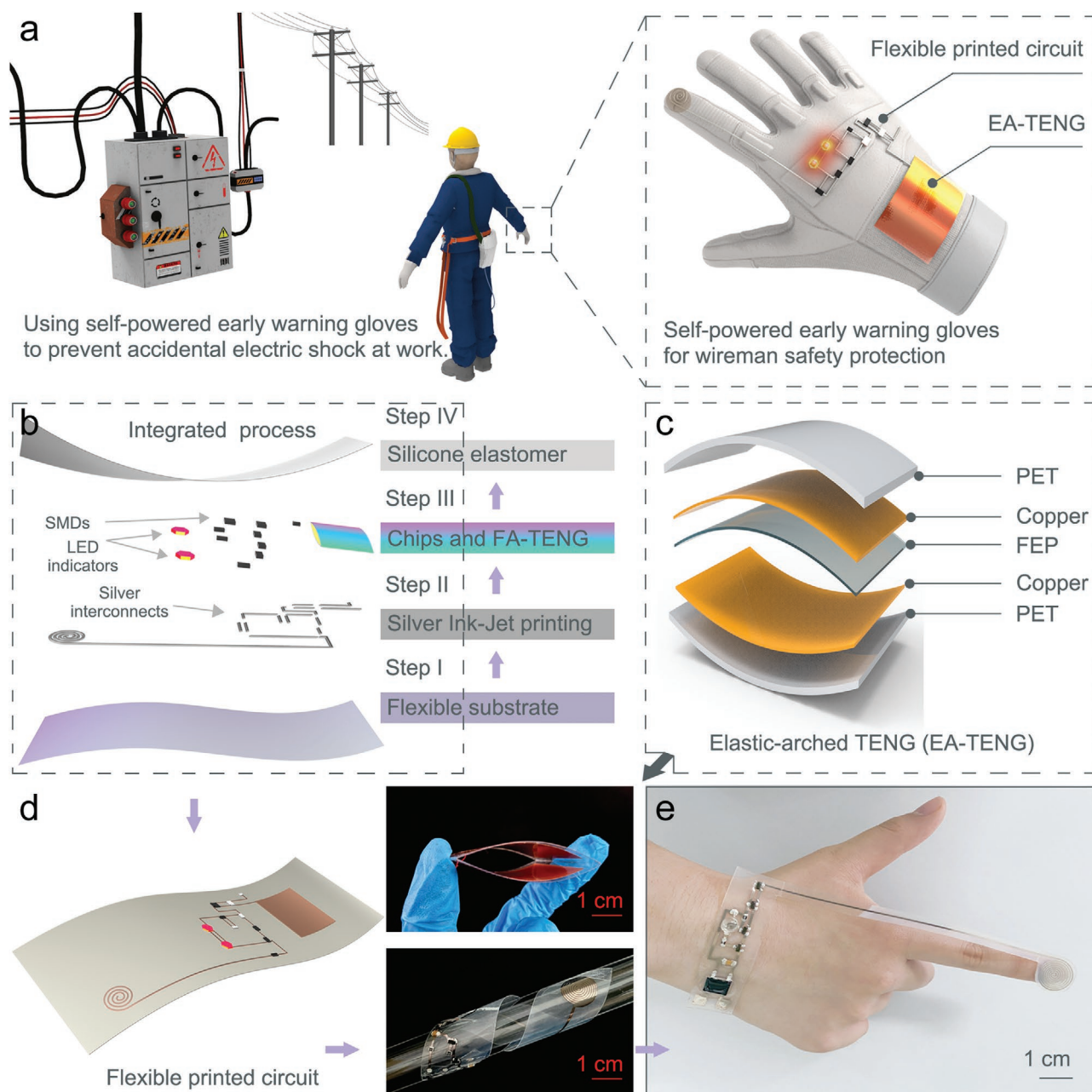
Figure 1. Overview of design and typical application scene of the SEWG. a) The typical scene of SEWG to protect engineer from getting an electric shock, and the design of SEWG for optimizing signal acquisition. b) The schematic illustration of flexible printed circuit integration process. c) An exploded view of structure of the EA-TENG based on contact-separation mode. d) The flexible circuit of the SEWG incorporates two working modules: i) energy harvesting module (right top), and ii) signal acquisition and alarm module (right bottom). e) The optical photo of the flexible printed circuit attached to the hand can be deformed with the movement of the hand.

electric output signals will be produced. Corresponding simulations of potential distributions in three different working states by COMSOL are shown in Figure 2b to observe the electricity generating process. The simulation results are in good agreement with the actual test data, and more detailed simulation parameters are shown in Figure S1, Supporting Information. In addition, the detailed working principle of the circuit for electrostatic and AC voltage detection will be explained in Section 2.5.

2.3. Electrical Output Performance of the EA-TENG

To characterize the output performance of the EA-TENG, we fix the EA-TENG with a contact area of 40×50 mm^2 on the acrylic board using a linear motor to provide periodic tapping motion and the results shown in Figure 2c–e. The output performance of the open-circuit voltage (V_{OC}), short-circuit current (I_{SC}), and transferred charges ($\triangle Q_{SC}$) of the TENG are 26 V (peak to peak), 1.25 µA, and 11.5 nC, respectively,
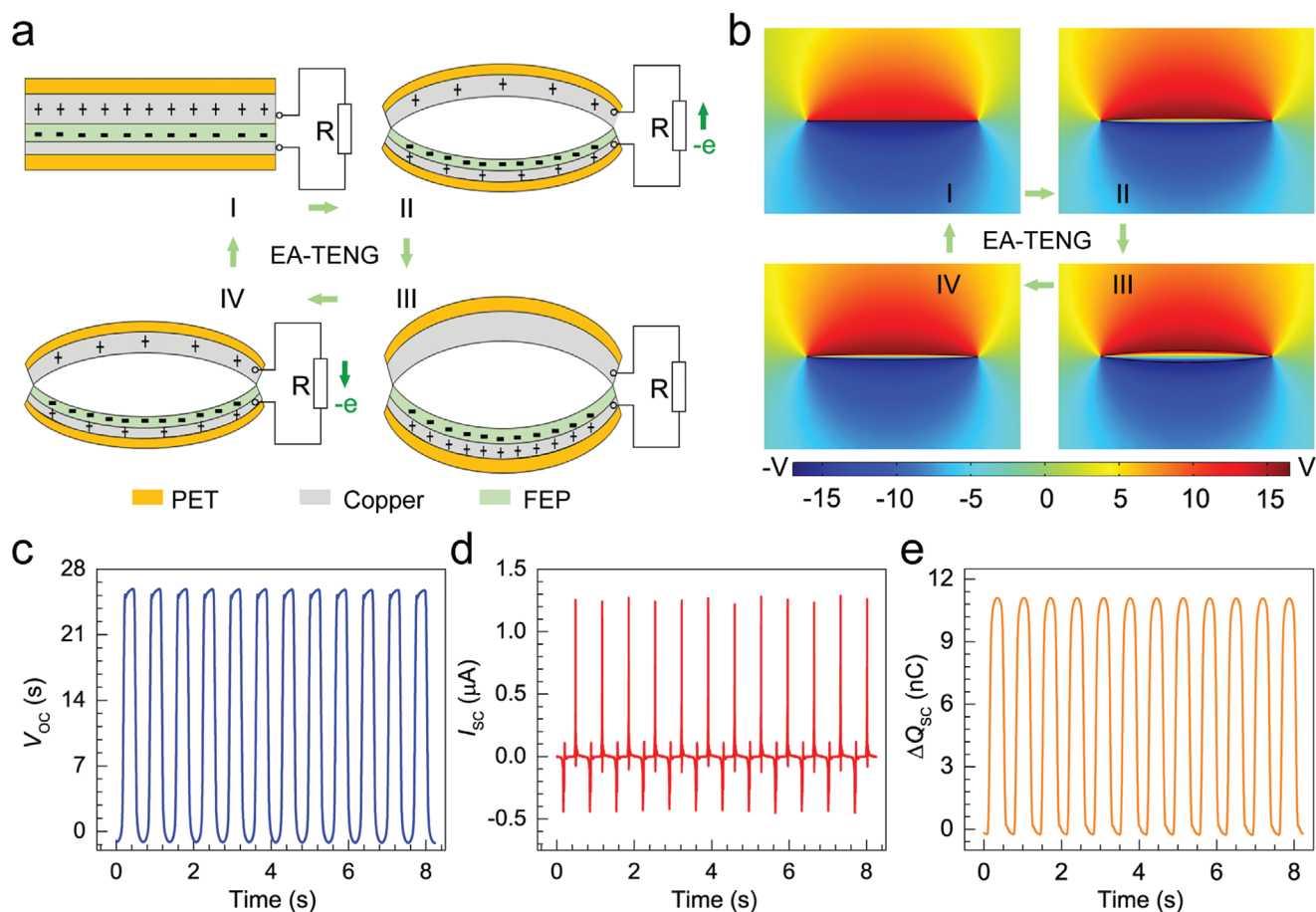
Figure 2. Working mechanism and basic output performance of the EA-TENG. a) Schematics of the operating principle for the EA-TENG. b) Potential simulation by COMSOL to elucidate the working principle. c–e) Open-circuit voltage, short-circuit current, and transferred charges of the EA-TENG.

and its surface charge density can be calculated as 5.75 µC m^{-2}.

In order to find the optimal geometry structure of the EA-TENG, we have analyzed the effect of the arrangement of the EA-TENG array on the output performance. The EA-TENG (i.e., electrode layer and dielectric layer) is sliced into different number of pieces (1, 2, and 4 pieces) under the condition that the contact area (40×50 mm^2) is guaranteed. Finally, they are connected together in parallel. The output performance of the V_{OC} and I_{SC} increases gradually with the decreasing of number of arrays (**Figure 3**a,b), and that is because every single TENG has its own amplitude and phases output character. When an entire piece of TENG is divided into an array structure, there are several air gaps between the different TENGs. Owing to the edge effects, the electric fields at the edge of the array cancel each other out thereby limiting the total output power of the array structure of TENGs.[33] Hence, the output efficiency has a phenomenon that $1 + 1$ is less than 2. The output performance of the TENG can be maximized only by finding the optimal location of the gap between the arrays. Besides, the TENG cut into arrays may be misplaced during contact separation process, resulting in a drop in the contact area and a lower output than the original whole block. The ambient condition is an important factor that affects the output performance of the EA-TENG, the effect of different temperature and relative humidity (RH) on the output

performance is studied. The V_{OC} and Q_{SC} of EA-TENG is measured in temperature varies from 293 to 323 K and humidity from 30% RH to 60% RH in an enclosed box. The influence of humidity on the EA-TENG is shown in Figure 3c,d, it can be noticed that the overall output performance shows a downward trend. The voltage has almost no attenuation before 50% RH and has the largest value of 24 V at 30% RH. Meanwhile, the transferred charges have only slight decrease after 30% RH, and then the output remains at same level. The relationship between the output performance of EA-TENG and temperature is shown in Figure 3e,f. It is found that the voltage decreases gradually with a continuous increase in temperature, but the transferred charges increase at the same time, which leads to the performance of EA-TENG almost unchanged. The results are consistent with previous studies that there is little effect on the output of TENG at temperatures below 353 K.[34] Considering the durability as shown in Figure 3g, the transferred charges only have a little decay in continuous operation of 80 000 cycles, confirming superior stability of our EA-TENG.

2.4. Fabrication Process of the SEWG

In order to make great integrated with wearable gloves, the circuit is manufactured to flexible form. The process of
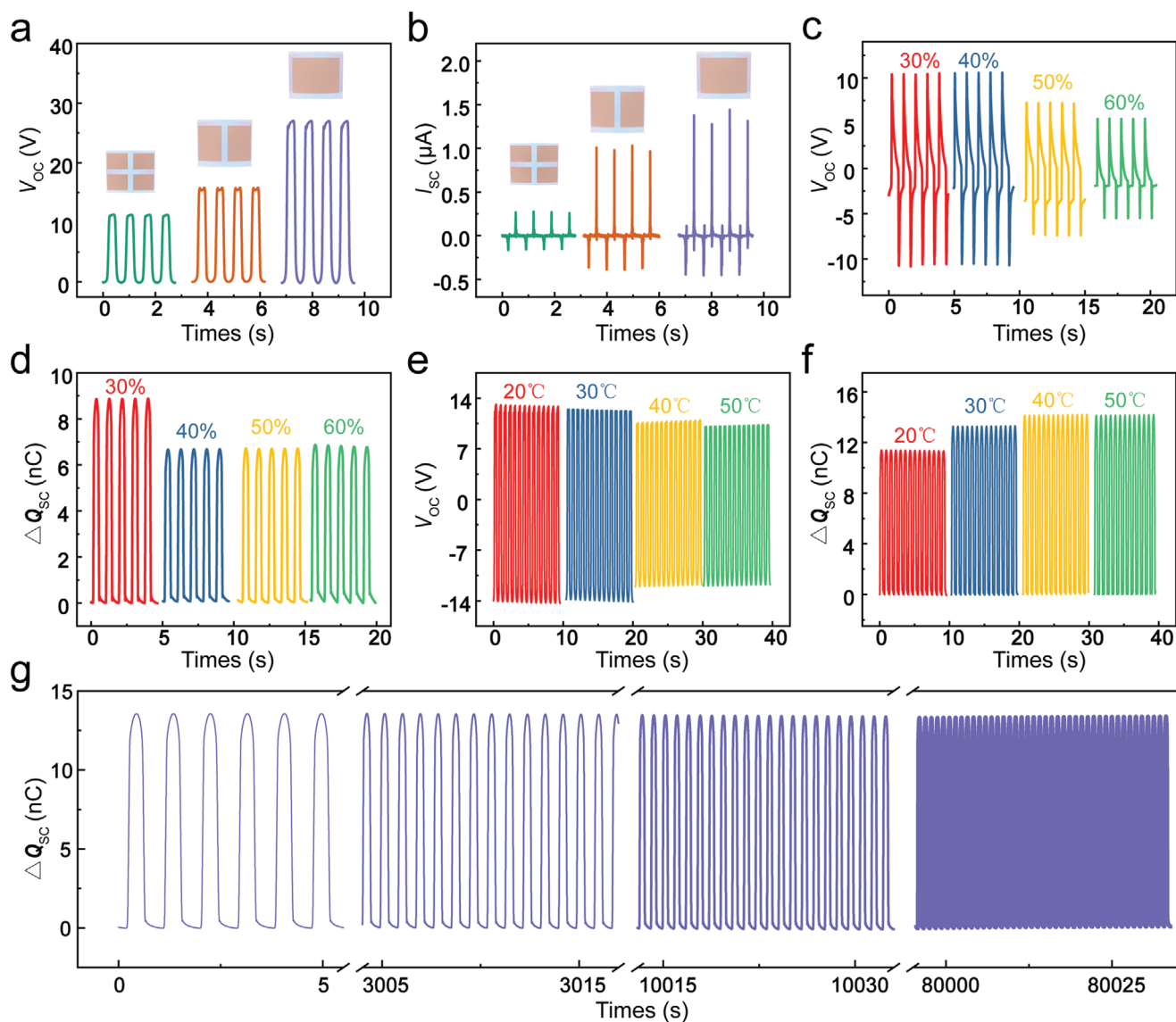
Figure 3. Electrical output and stability of the EA-TENG. a,b) Open-circuit voltage and short-circuit current of different array numbers of the electrodes and dielectric layers for the EA-TENG. c,d) Effects of the environment humidity on c) open-circuit voltage and d) transferred charge of the EA-TENG. Effects of the environment temperature on e) open-circuit voltage and f) transferred charge of the EA-TENG. g) Stability and robustness measurement of the EA-TENG, where the transferred charges were recorded for over 80 000 cycles at a frequency of 1 Hz.

manufacturing a flexible circuit with inkjet printing technology is illustrated in **Figure** 4a. Firstly, the circuit is designed in Altium Designer software and output its Gerber files saved as PDF files which need to be transferred to bit map file (TIFF) in the end. Then the picture can be recognized by Printing machine and print the pattern with ink made of silver nanoparticles on PET substrate. The size of each drop of ink is about 3.5 pl, and the minimum thickness after sintering is 123.3 nm (Figure S2, Supporting Information). The inks contain organic additives added to enhance printability, which is insulating, so a post-processing step called sintering is required to melt organic material. After the sintering process finish at 150 °C for 20 min, the printed silver wires will be able to provide continuous electron transport pathways. Using a needle tube to carefully apply conductive silver glue to the electrode pads, we pasted

the discrete components to prototype circuit and then put it to thermostatic drying oven. The flexible circuit is equipped with control function after heating the silver glue for 5 min at 45 °C. Furthermore, the circuit is to be packaged with silicone elastomer in order to make an effect on strengthening connection between components and electrode pad. The optical photo of the fabricated flexible circuit before packaging is shown in Figure 4b. Contrasting after inkjet printing, an enlarged optical micrograph of printed structures in Figure 4c shows a well-connected silver-ink trail after sintering. After that, we characterized the mechanical properties of the flexible printed circuit, and the results are shown in Figure 4d,e. The circuit before and after heating at 45 °C for 12 h bent with a device, and the bending angle was about 60°. The resistance of the printed sliver trace (T1, Black) and the conductive silver glue between printed silver
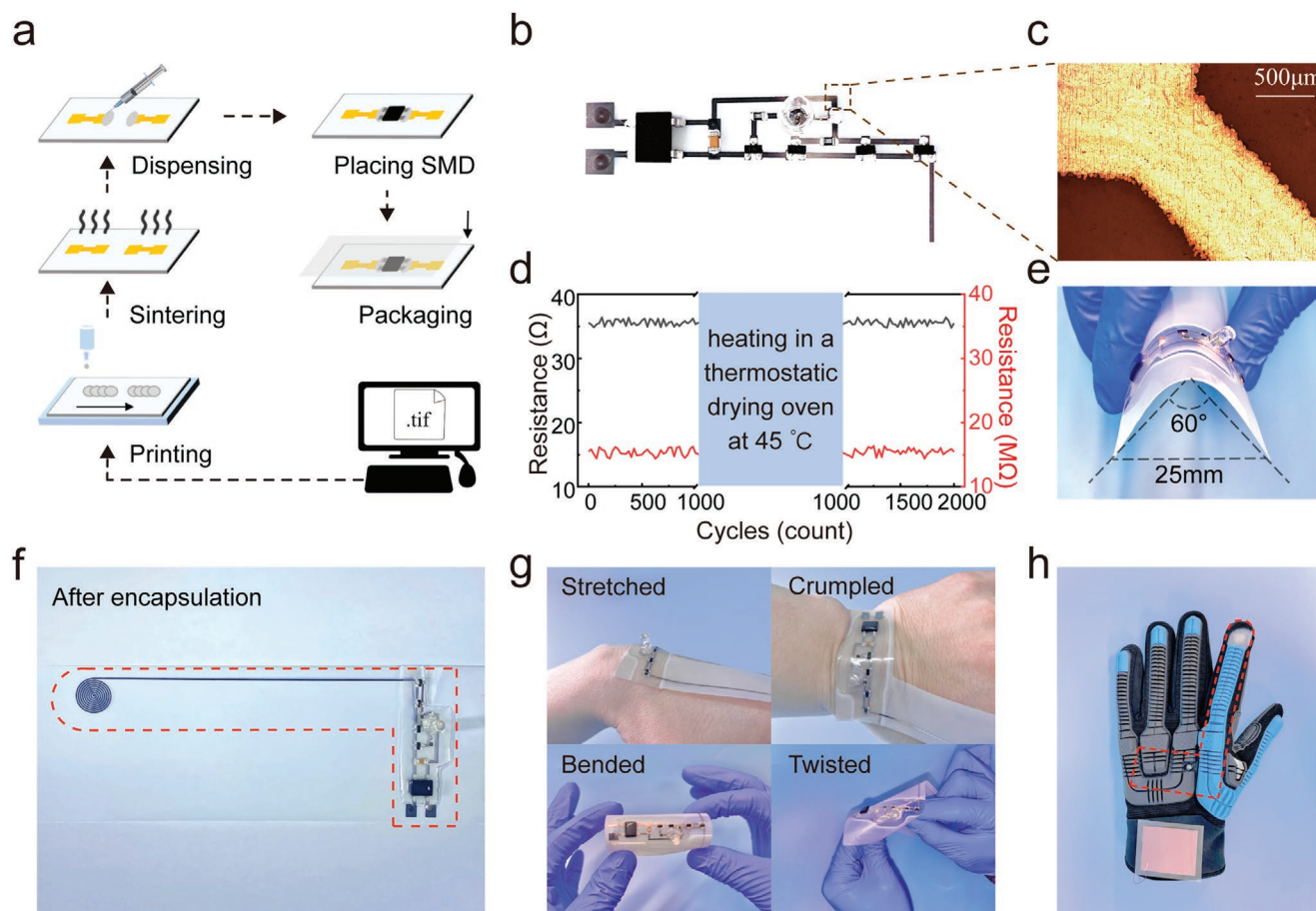
Figure 4. Fabrication of SEWG and mechanical properties. a) The manufacturing operation of flexible printed circuit. b,c) The optical photo of the fabricated flexible circuit before packaging and an enlarged optical micrograph of printed circuit trace. d,e) The mechanical properties of the flexible printed circuit and the angle of bending test is 60°. f) The flexible printed circuit that is packaged with silicone elastomer. g) Optical images of the flexible circuit stretched around the wrist, crumpled on the skin, bended, and twisted. h) The SEWG, which integrates the flexible printed circuit and EA-TENG, has the function of self-powered electrical signal detection.

wire-pad (S1, Red) are mechanically cycled for 2000 cycles and negligible change in the electrical resistance is observed. The access status of LCR is provided in Figure S3, Supporting Information. Cutting the packaged circuit into the shape of a finger along the set route (Figure 4f), the circuit can stand many kinds of shape change that can be stretched (Figure 4g, top left), crumpled (Figure 4g, top right), bended (Figure 4g, bottom left), and twisted (Figure 4g, bottom right). At last, the packaged flexible circuit and the EA-TENG are both integrated to commercial gloves shown in Figure 4h. The SEWG is designed suitable to gloves size and this kind of integration is not only convenient for performing the gloves' function but also perfectly matched hand's activity.

2.5. Applications of the SEWG for Electric Shock Protection

Figure 5a shows the basic structure of circuit. The upper figure shows the power produced by EA-TENG is accumulated to a capacitor through a full-wave bridge before starting the detection and then the capacitor supplies the energy to complete a detection for once as the nether figure shows. The capacitor

is chosen to endure high voltage in case to avoiding breaking down and the value should be suitable small for getting sufficient voltage to drive the circuit in a short time. The voltage between two ends of the capacitor can be expressed:

$$V = \frac{Q_{sc}}{C} \tag{1}$$

The transistors, on the one hand are used to avoid the mis-detection by utilizing the threshold voltage V_{be}, and the threshold voltage can be expressed as:

$$V_{th} = V_{be}\big|_{tr_1} + V_{be}\big|_{tr_2} + V_{be}\big|_{tr_3} + V_{be}\big|_{tr_4} \tag{2}$$

As four transistors are the same, the V_{th} can be calculated to 4 V_{be}. On the other hand, it can be used to amplify the current through the led. Supporting the base electrode current of transistor tr_1 is I_b and the gain of the transistors is β, the instant current I flow through led can be expressed as:

$$I = (1+\beta)^4 \cdot I_b \tag{3}$$

**ADVANCED
SCIENCE NEWS**
www.advancedsciencenews.com

**ADVANCED
MATERIALS
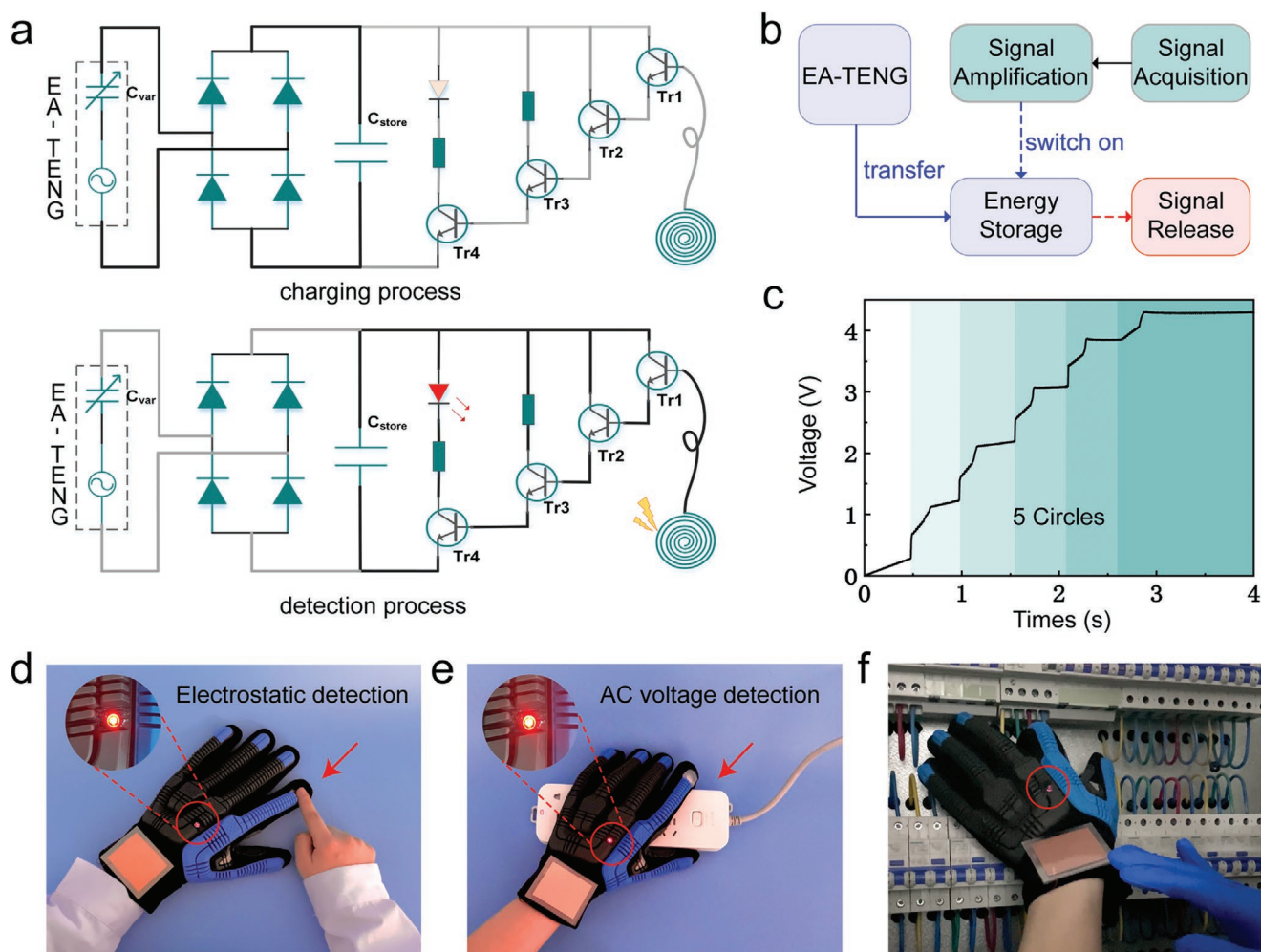TECHNOLOGIES**
www.advmattechnol.de

Figure 5. Applications of the SEWG. a) The basic structure of the circuit and the state of the different working processes. b) System-level block diagram shows the working principle of SEWG. c) The charge curve of capacitor storage, the accumulated capacitance voltage reaches 4 V within 3 s. d) The electrostatic detection process of human body. e) The AC voltage detection process in wire of a power outlet. f) Scene diagram of mechanical energy collection and live voltage detection in the low tension distribution box by using SEWG.

The LED will send an alarm signal when the bias voltage of transistor tr_1 induced by the electrostatic charge or alternating current at the inductor is higher than threshold voltage 4 V_{be}. Besides this, the voltage of C_{store} also should be high enough to drive the circuit, and the condition is:

$$V_{c_{store}} \geq 4V_{be} + V_{diode} \tag{4}$$

where the $V_{c_{store}}$ means the voltage of C_{store}, the V_{diode} means the threshold voltage of LED.

In general, the working process of the SEWG is divided into three parts: the body's energy harvesting, the acquisition of electrical signals, and the amplified signals release the stored energy to light the warning LED (Figure 5b). Through the Oersted experiment, it can be known that a conductor carrying an AC voltage produces a varying magnetic field around it. The antenna of circuit which is energized by the phenomena of electromagnetic induction, produces a small amount of current in it. The transistors not only amplify the current but also act as switches. Figure 5c shows the charge

curve of the storage capacitor. It can be noticed that the voltage of the capacitor rises corresponding to the pressing numbers of EA-TENG and it reaches more than 4 V after 5 times press. As the V_{diode} is about 0.7 V and the threshold voltage of diode is 0.7 V around, the capacitor's voltage should be charged higher than 3.5 V. The applications of SEWG are shown in Figure 5d–f and it is used for human electrostatic detection, AC current detection, and distribution electric box detection. Press EA-TENG fixed on gloves first, and then the alarm signal will be sent when the inductor electrode contacts with human body as Figure 5d shows. The reason is that static electricity from human body supplies a bias voltage for triggering the transistors. The bias voltage can also be induced by AC current in wire when inductor electrode gets close to the wire as Figure 5e shows. Figure 5f shows a typical application scene that the engineer easily ignored the danger existed on distribution electric box while examining the wire problems, and it can give a convenient detection as well as striking alarm to engineer which provides an indispensable protection.

**ADVANCED
SCIENCE NEWS**

www.advancedsciencenews.com

**ADVANCED
MATERIALS
TECHNOLOGIES**

www.advmattechnol.de

3. Conclusion

In summary, a SEWG has been demonstrated which is composed of the contact-separation mode EA-TENG, flexible printed circuit, and a pair of insulate gloves. This unique self-powered device overcomes the limitations of convention wearable electronics that require an external power supply and has the ability of anti-electric shock for human safety protection. Firstly, the EA-TENG generates electricity from a continuous touch lightly by hand or body, and as a sustainable self-powered source that the V_{OC} and I_{SC} can reach to 26 V (peak to peak), 1.25 µA under an external mechanical trigging, respectively. For this SEWG, it can be utilized to complete one charging process by simply five times slapping, which lay the foundation for the SEWG to be utilized in practice. In addition, the SEWG has the unique advantage that can really deliver real-time no-contact electrostatic monitoring when no external power is supplied, and can effectively avoid the electric shock accident in 220/380 V electric maintenance work. Furthermore, quantitative analyses of the mechanics and electronics characteristics of the SEWG demonstrate advantages in stability and reliability, which there is always a well performance when is operated more than 80 000 working cycles. Most importantly, it has been demonstrated that the glove is able to provide no-contact early warning feedback for AC circuit or on a live wire, and has sufficient detection range to avoid the direct contact with an energized conductor. Therefore, SEWG has excellent ability of self-powered early warning, which means that SEWG has made a breakthrough in the combination of bio-energy harvesting and self-powered environment interaction. This work not only shows the design is reliable for practical applications, but also a new approach for self-powered wearable electronic field in the near future.

4. Experimental Section

Fabrication of the TENG: The fabrication process started with the preparation of the electrode and dielectric layer materials. 80 µm thick FEP was chosen as the dielectric layer and 20 µm thick copper foil as the electrode (both with back glue). The FEP was tightly affixed to the fixed copper foil to prevent the formation of air bubbles. After the film made in the previous step was cut to the appropriate shape, it was pasted on the PET substrate (150 µm), and the thin wire was clamped on the reserved position. Similarly, a piece of copper foil and wire would be attached to the PET substrate as the other half of the elastic-arched TENG.

Fabrication of the Flexible Circuit Board: The circuit was designed by Altium Designer 16, and then outputted and transferred to bit map file. The picture was printed by flexible circuit printer DP500. The basement of the circuit board was PET and the conductive wire was nano silver ink. The soft solder used to paste the discrete components was NC-576 and the infrared IC heater was T-962.

Measurement: The humidity was controlled by a humidifier, the temperature was provided by an electric heater, and stabilized for more than 1 h. A step motor (LinMot E1100) was applied to provide the periodic contact-separation movement for the TENG. For the section of basic output performance tests of EA-TENG, several programmable electrometers (6517 from Keithley Instruments) were directly linked to a synchronous data acquisition card (6356 from National Instruments) to simultaneously measure the multichannel open-circuit, voltage (V_{OC}), short-circuit current (I_{SC}), or transferred charge ($\triangle Q_{SC}$) signals. These data were collected and saved by a corresponding multichannel data acquisition program which was developed on the LabVIEW platform.

Control parameters such as acceleration (0.15 m s^{-2}), frequency (1.5 Hz), and maximum movement distance (7 mm) were set to the linear motor. In the mechanical performance test section, resistance was measured by LCR instrument (Agilent 4263B).

Supporting Information

Supporting Information is available from the Wiley Online Library or from the author.

Conflict of Interest

The authors declare no conflict of interest.

Data Availability Statement

Research data are not shared.

[1] M. J. Cima, *Nat. Biotechnol.* **2014**, *32*, 642.

[2] M. Ha, J. Park, Y. Lee, H. Ko, *ACS Nano* **2015**, *9*, 3421.

[3] D. Son, J. Lee, S. Qiao, R. Ghaffari, J. Kim, J. E. Lee, C. Song, S. J. Kim, D. J. Lee, S. W. Jun, S. Yang, M. Park, J. Shin, K. Do, M. Lee, K. Kang, C. S. Hwang, N. Lu, T. Hyeon, D. H. Kim, *Nat. Nanotechnol.* **2014**, *9*, 397.

[4] M. L. Hammock, A. Chortos, B. C. Tee, J. B. Tok, Z. Bao, *Adv. Mater.* **2013**, *25*, 5997.

[5] E. Dolgin, *Nature* **2014**, *511*, S16.

[6] R. Herbert, J. H. Kim, Y. S. Kim, H. M. Lee, W. H. Yeo, *Materials* **2018**, *11*, 187.

[7] B. Zhang, Y. Tang, R. Dai, H. Wang, X. Sun, C. Qin, Z. Pan, E. Liang, Y. Mao, *Nano Energy* **2019**, *64*, 103953.

[8] M. K. Choi, J. Yang, K. Kang, D. C. Kim, C. Choi, C. Park, S. J. Kim, S. I. Chae, T. H. Kim, J. H. Kim, T. Hyeon, D. H. Kim, *Nat. Commun.* **2015**, *6*, 7149.

[9] Y. Gao, L. Yu, J. C. Yeo, C. T. Lim, *Adv. Mater.* **2020**, *32*, 1902133.

[10] G. Schwartz, B. C. Tee, J. Mei, A. L. Appleton, D. H. Kim, H. Wang, Z. Bao, *Nat. Commun.* **2013**, *4*, 1859.

[11] S. Xiang, D. Liu, C. Jiang, W. Zhou, D. Ling, W. Zheng, X. Sun, X. Li, Y. Mao, C. Shan, *Adv. Funct. Mater.* **2001**, *31*, 2100940.

[12] Y. Wang, C. Yan, S. Y. Cheng, Z. Q. Xu, X. Sun, Y. H. Xu, J. J. Chen, Z. Jiang, K. Liang, Z. S. Feng, *Adv. Funct. Mater.* **2019**, *29*, 1902579.

[13] H. Abdolmaleki, P. Kidmose, S. Agarwala, *Adv. Mater.* **2021**, *33*, 2006792.

[14] M. Gao, P. Wang, L. Jiang, B. Wang, Y. Yao, S. Liu, D. Chu, W. Cheng, Y. Lu, *Energy Environ. Sci.* **2021**, *14*, 2114.

[15] W. Liu, Z. Wang, G. Wang, G. Liu, J. Chen, X. Pu, Y. Xi, X. Wang, H. Guo, C. Hu, Z. L. Wang, *Nat. Commun.* **2019**, *10*, 1426.

[16] N. Zhang, C. Qin, T. Feng, J. Li, Z. Yang, X. Sun, E. Liang, Y. Mao, X. Wang, *Nano Research* **2020**, *13*, 1903.

[17] A. Nathan, A. Ahnood, M. T. Cole, L. Sungsik, Y. Suzuki, P. Hiralal, F. Bonaccorso, T. Hasan, L. Garcia-Gancedo, A. Dyadyusha, S. Haque, P. Andrew, S. Hofmann, J. Moultrie, C. Daping, A. J. Flewitt, A. C. Ferrari, M. J. Kelly, J. Robertson, G. A. J. Amaratunga, W. I. Milne, *Proc. IEEE* **2012**, *100*, 1486.

[18] C. Cheng, X. Li, G. Xu, Y. Lu, S. S. Low, G. Liu, L. Zhu, C. Li, Q. Liu, *Biosens. Bioelectron.* **2021**, *172*, 112782.

[19] M. Wang, J. Zhang, Y. Tang, J. Li, B. Zhang, E. Liang, Y. Mao, X. Wang, *ACS Nano* **2018**, *12*, 6156.

[20] W. Liu, Z. Wang, C. Hu, *Materials Today* **2021**, *45*, 93.

[21] S. Wang, L. Lin, Z. L. Wang, *Nano Lett.* **2012**, *12*, 6339.

[22] C. Xu, Y. Song, M. Han, H. Zhang, *Microsyst. Nanoeng.* **2021**, *7*, 25.

[23] X. Pu, H. Guo, J. Chen, X. Wang, Y. Xi, C. Hu, Z. L. Wang, *Sci. Adv.* **2019**, 30.

[24] P. Chen, J. An, S. Shu, R. Cheng, J. Nie, T. Jiang, Z. L. Wang, *Adv. Energy Mater.* **2021**, *11*, 2003066.

[25] F. Liu, Y. Liu, Y. Lu, Z. Wang, Y. Shi, L. Ji, J. Cheng, *Nano Energy* **2019**, *56*, 482.

[26] B. Chen, W. Tang, T. Jiang, L. Zhu, X. Chen, C. He, L. Xu, H. Guo, P. Lin, D. Li, J. Shao, Z. L. Wang, *Nano Energy* **2018**, *45*, 380.

[27] J. Wang, S. Li, F. Yi, Y. Zi, J. Lin, X. Wang, Y. Xu, Z. L. Wang, *Nat. Commun.* **2016**, *7*, 12744.

[28] Y. Zou, P. Tan, B. Shi, H. Ouyang, D. Jiang, Z. Liu, H. Li, M. Yu, C. Wang, X. Qu, L. Zhao, Y. Fan, Z. L. Wang, Z. Li, *Nat. Commun.* **2019**, *10*, 2695.

[29] L. Yin, K. N. Kim, J. Lv, F. Tehrani, M. Lin, Z. Lin, J. M. Moon, J. Ma, J. Yu, S. Xu, J. Wang, *Nat. Commun.* **2021**, *12*, 1542.

[30] Z. Wang, J. An, J. Nie, J. Luo, J. Shao, T. Jiang, B. Chen, W. Tang, Z. L. Wang, *Adv. Mater.* **2020**, *32*, 2001466.

[31] J. Luo, Z. Wang, L. Xu, A. C. Wang, K. Han, T. Jiang, Q. Lai, Y. Bai, W. Tang, F. R. Fan, Z. L. Wang, *Nat. Commun.* **2019**, *10*, 5147.

[32] Y. Tang, H. Zhou, X. Sun, N. Diao, J. Wang, B. Zhang, C. Qin, E. Liang, Y. Mao, *Adv. Funct. Mater.* **2019**, 30.

[33] J. Shao, Y. Yang, O. Yang, J. Wang, M. Willatzen, Z. L. Wang, *Adv. Energy Mater.* **2021**, *11*, 202100065.

[34] S. Lin, L. Xu, C. Xu, X. Chen, A. C. Wang, B. Zhang, P. Lin, Y. Yang, H. Zhao, Z. L. Wang, *Adv. Mater.* **2019**, *31*, 1808197.